Proceeding of 2nd International Science Postgraduate Conference 2014 (ISPC2014)

COLUMN STUDY OF HUMIC ACID REMOVAL FROM WATER ONTO SURFACTANT MODIFIED GRANULAR ZEOLITE

[1]AWAD F.ELSHEIKH, [2] UMI KALTHOM AHMAD AND [3] ZAINAB RAMLI

[1,2,3]Department of Chemistry Sciences, Faculty of Science
Universiti Teknologi Malaysia,
81310 UTM Johor Bahru, Johor, Malaysia

[1]awad2003@yahoo.com, [2*]umi@kimia.fs.utm.my, [3]zainb@kimia.fs.utm.my

*Corresponding author

Abstract. Abstract. In this study, natural zeolite (mordenite) was modified by using dimethyldioctadecylammonium bromide (DDAB) with polyvinyl alcohol (PVA) to afford surfactant modified granular zeolite (SMGZ) as adsorbent for humic acid (HA) removal. Column adsorption studies were carried out to examine the optimum conditions for the removal of HA by SMGZ. The optimum loading of surfactant was later utilized in characterization studies. The SMGZ were characterized by XRD, FTIR, BET specific surface area and FESEM. The removal of HA was performed in a fixed bed reactor. The effects of different experimental parameters such as DDAB loading levels, solution pH and HA solution flow rate were evaluated. Samples were collected and analyzed using UV. The results indicated that SMGZ showed great enhanced adsorption capacity of HA compared to natural granular zeolite due to the hydrophobic interaction and hydrogen bonding. The equilibrium uptake ($q_{eq(exp)}$) of HA decreased with increasing, flow rate and granular size. Total removal percent (Y) of HA SMGZ was found to increase with increasing solution pH, influent concentration and bed depth.

Keywords Humic acid removal; surfactant modified granular zeolite; fixed bed reactor.

1.0 INTRODUCTION

Humic acid (HA) is one of the main components of humic substances (HS) within what knows natural organic matter (NOM). HA are a heterogeneous class of moderate molecular weight, yellow-colored bio-molecules existing commonly in all soils, sediments, and natural waters. HA derived from living and dead plants, animals and microorganism, their waste products and from degradation of these sources [1,2]. The HA are not directly toxic in water but have undesirable effects on the appearance, which changes the color of the waters from yellow to brown, and taste of water and are very hazard in water treatment processes [3]. Since the early 1970s, water quality and treatment issues related to HA have been reported, where these substance in natural water facilitating bacteria reproduction during drinking water distribution, produces carcinogenic disinfection byproducts (DBP) during chlorination process, such as trihalomethanes (THMs), and it has been known that the HAs have an effect on the fate of micro-organic pollutants (e.g. intake, accumulation, movement, degradation, toxicity, etc.) [4]. Recent discovery of HA being one reason for Kaschin-Beck and other diseases brought new notice to the removal of HA in the water [5 and 6].

A large number of epidemiological studies since 1974 have repeatedly shown the existence many of DBPs in water supply are usually present at low concentration, but may further to potential human health risks due to exposure to low levels of DBPs over long periods of time through the different uses of chlorinated water and many of the DBPs have been classified as probable or possible carcinogens, and mutagenic [7]. Therefore, it is of great importance to remove HA from drinking water.

To remove HA during water treatment, a enormous assortment of processes have been developed, such as coagulation/flocculation, membrane separation, advanced oxidation, ion-exchange and adsorption [8–12]. Among these methods, adsorption has been considered as a successful method because of its ease of design, simplicity of process and high effectiveness [13]. Activated carbon is a common adsorbent for removing pollutants from water [14]. Though, activated carbon is not very effectual in adsorption large molecules such as HA from water due to its micropores are inaccessible for HA [15]. Newly, there is a

great concern in development of novel adsorbents for effectual removal of HA from water [1–14].

Natural zeolites are crystalline microporous aluminosilicates with very well distinct structures that consist of a framework shaped by tetrahedrons of SiO_4 and AlO_4, and they have permanent negative charge in their crystal structures that can be balanced by exchangeable cations such as Ca^{2+}, Mg^{2+}, K^+ and Na^+. Thus, natural zeolites typically can exchange cations but not anions, which making them suitable for surface modification using cationic surfactants. Previously, natural zeolite was improved by surfactants to increase adsorption and removal of HA from water such as hexadecyltrimethylammonium-bromide (HDTMA), n-cetylpyridinium (CPD), benzyltetradecyl ammonium (BDTDA), stearyldimethylbenzylammonium (SDBAC) [16].

There are eight industrial zeolite minerals recognized: clinoptilolite, mordenite, phillipsite, chabazite, erionite, ferrierite, laumontite and analcime. [17,18]. Mainly those of mordenite in China, has initiated great attention in the use of mordenite in water treatment. Mordenite is a high silica zeolite. Its typical unit cell formula is $Na_8[(AlO_2)_{40}(SiO_2)_{40}].24H_20$. Mordenite is gradually more being utilization as a molecular sieve in the adsorptive separations of liquid mixtures involving acidic components; it also finds wide application as a catalyst for water treatment. The mordenite kind having a high silica/alumina ratio is favored for use at relatively higher temperatures and where acidic components are involved [19]. Lately it has been established that mordenite is an effectual denote to remove pollutant molecules from water [20].

Recent studies have confirmed the ability of powdered zeolites as successful adsorbents for the removal of HA from water [21-23]. On the other hand, the high friction loss related with passing water through powder beds prevents applies of powdered adsorbents in treatment systems. Few researches have directly evaluated granular zeolites in fixed-bed reactors [24]. In this work, the efficiency of several surfactant modified granular zeolites (SMGZ) by using dimethyldioctadecylammonium bromide (DDAB) with polyvinyl alcohol (PVA) to the removal of HA from water was evaluated. In addition, the equilibrium and kinetic parameters that describe the adsorption of HA onto SMGZ were determined.

2.0 EXPERIMENTAL

2.1 Materials and Instruments

The mordenite sample (natural zeolite) used in the experiments was imported and distributed in Malaysia by Chan Chun Chan Enterprise Company. The particle size distribution of powder natural zeolite was adjusted ≤ 425 µm standard England mesh. The cation exchange capacity (CEC) of natural zeolite was determined to be 108.3 meq/100g while the external cation exchange capacity (ECEC) is 0.456 meq/g. The reagents used for modified zeolite were DDAB as cationic surfactant which was supplied by ACROS ORGANICS, USA and PVA from Merck, Germany. HA from Molekula was used as biodegradation of NOM. A Perkin Elmer UV-vis spectrophotometer (Lambda 25, USA) was used to determine HA concentration at λ_{max} = 254nm.

2.3 Preparation of Surfactant Modified Granular Zeolite

Based on Shams and Mirmohammadi method, natural zeolite powder mixed with a required weight of surfactant (DDAB) in beaker 500ml and 250 ml distilled water. The mixture was stirred with a magnetic stirrer till thick slurry was prepared and shaker at 175 rpm for 24 h. The samples of surfactant modified powder zeolite are separated by simple filtration and washed by distilled water and dried at 60°C for 24h. About 1 weight percent of the dried SMZ of low molecular weight polyvinyl alcohol (PVA) was dissolved in distilled water and added to the previously prepared powder, and the blend was homogenized by spatula to form paste. The paste was passed through a home-made extruder whose schematic is exposed in **Figure 2.1**. The spaghetti-like noodles were semi-dried at room temperature for 24h (**Figure 2.2a**). The dried noodles was then crushed and by passing through standard ASTM sieves, the particle size distribution of all samples of surfactant modified granular zeolite (ZMGZ) was adjusted 0.4-30.35 mm standard England mesh (**Figure 2.2b**). In this work seven samples of SMGZ were prepared consistent with the compositions reported in **Table 2.1**.

Table 2.1: Composition of natural zeolite, surfactant and binder in paste samples.

Sample	Natural zeolite (%)	Surfactant (%)	Binder (PVA) (%)
S1	99	00	1
S2	95	4	1
S3	91	8	1
S4	87	12	1
S5	83	16	1
S6	79	20	1
S7	75	24	1

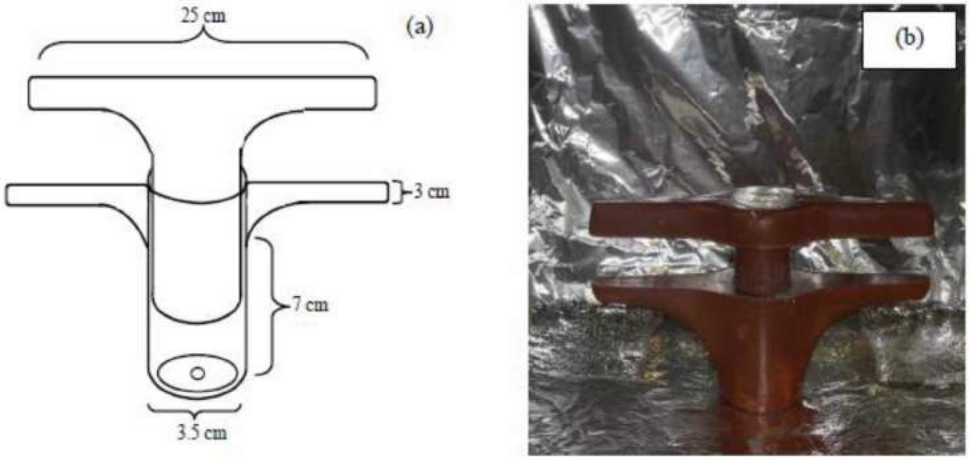

Figure 2.1: Schematic (a) and picture (b) of the manual homemade extruder.

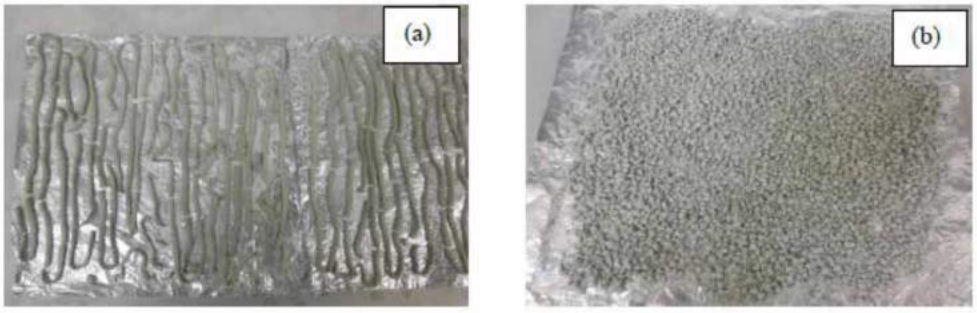

Figure 2.2: Picture of (a) The spaghetti-like noodles and (b) SMGZ.

2.4 Humic acid adsorption Studies

The laboratory-scale investigational system consists of zeolite fixed-bed column, HA solution conical flask, peristaltic pump (MASTER FL 77240-10), flowmeter, valves and water tank (**Figure 2.3**).

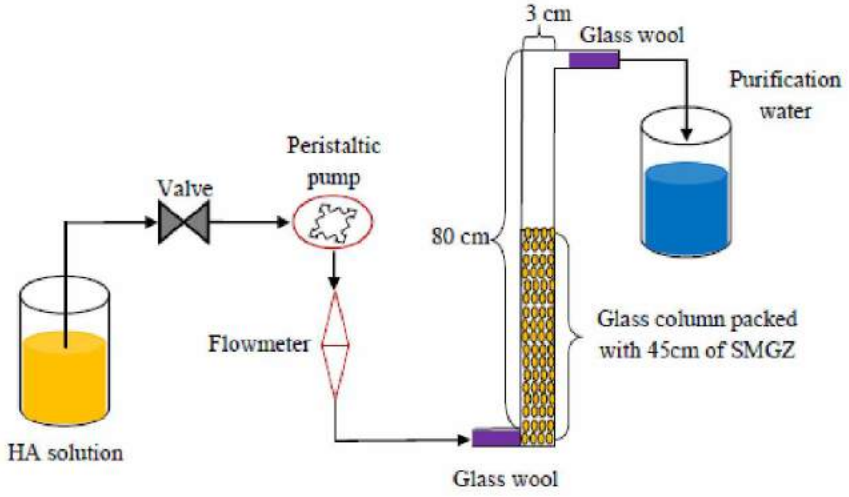

Figure 2.3 The schematic flow sheet of fixed-bed

The packed column has a height of 80 cm and internal diameter of 3 cm. The particle size of mordenite was 0.4-3.35 mm with a bed height 45cm and filling weight of 150 g. Experimentations were implemented to identify the optimum loading level of DDAB for preparing modified granulate zeolite and subsequent removal of HA by surfactant modified granular zeolite (SMGZ) in the column reactor. The reactor is consists of a fixed-bed column to which HA solution is pumped from the HA solution tank to the bottom of the column. At the frits stage of test, a peristaltic pump was used to feed the HA solution (30 mg/L) to the bed filled with SMGZ with a desired loading of DDAB and PVA (**Table 2.2**) at flow rate of 18 ml/min. At the second step, determine the DDAB loading level and different parameters were examined. Samples were collected and analyzed against percent loading of DDAB of SMGZ for HA solutions. The concentrations of HA were determined at 254 nm. Amounts of the collected HA were calculated from the divided between influent and effluent concentrations and effluent time. The

effects of different experimental parameters such as solution pH, HA solution flow rate, influent concentration, granular size and bed depth were evaluated.

2.5 Mathematical column models

The effectiveness of a fixed-bed column is represented through the concept of the breakthrough curve. The time for breakthrough manifestation and the shape of the breakthrough curve are significant characteristics for defining the operation and the dynamic response of an adsorption column. The breakthrough curve (BC) represents the development of the solution concentration in function of adsorption parameters. The loading behavior of HA to be adsorbed from water in a column is defined in term of Ct /C0 as a function of time or volume of the effluent for a given bed height, giving a breakthrough curve [26].

The total weight of HA adsorbed by adsorbent in fixed-bed (q_{total}, mg) can be calculated from the breakthrough curve obtained use integrating the adsorbed HA concentration (C_{ad}, mg L^{-1}) versus time plot as equation (2.2) [27-30]:

$$q_{total} = \frac{Q}{1000} \int_{t=0}^{t= t_{total}} C_{ad}\, dt \qquad (2.1)$$

$$C_{ad} = C_0 - C_t \qquad (2.2)$$

$$q_{total} = \frac{Q}{1000} \int_{t=0}^{t= t_{total}} (C_0 - C_t)\, dt \qquad (2.3)$$

where Q is volumetric flow rate (mL min^{-1}), C_0 is influent HA concentration (mg L^{-1}), C_t is effluent HA concentration (mg L^{-1}), t is effluent time (min), t_{total} is total flow time (min). The equilibrium uptake is the weight of HA adsorbed per g of adsorbent from experiment (q_e, mg g^{-1}) is calculated from the following equation [27-30]:

$$q_e = \frac{q_{total}}{X} \qquad (2.4)$$

where X is total dry weight of zeolite in column (g). The total amount of HA sent to column (M_{total}, mg) is given as following [27-30]:

$$M_{total} = \frac{C_0 Q\, t_{total}}{1000} \qquad (2.5)$$

The total HA removal efficiency (Y, %) is the relation between the maximum capacity of the column to the total amount of HA sent to column as equation (2.6) [27-30]:

$$Y = \frac{q_{total}}{M_{total}} \times 100 \qquad (2.6)$$

3.0 RESULTS AND DISCUSSION

3.1 Characterization

3.1.1 XRD analysis

The investigation of natural zeolite (NZ) and SMGZ were carried out by XRD and compared their XRD data with each other. NZ sample may include a variety of other minerals such as quartz, montmorillonite and feldspar [31]. The XRD diffractograms of the NZ and SMGZ at different loading of DDAB can be seen in **Figure 3.1.** The quantitative analysis according showed that the NZ used in this study was mainly composed of mordenite (M) and quartz (Q). Quartz was detected as a major component in the NZ with 78.13% while mordenite gave only 21.86% based on the percentage of intensity peaks at I_{100} for mordenite and I_{100} for quartz (**Figure 3.1**). The model unit cell formula of natural zeolite mineral, mordenite, is given as Na_8 $[(Al_2O_3)4$ $(SiO_2)_{40}].24H_2O$ [19]. This demonstrates a silica/alumina ratio of 10:1. The XRD of the different loading capacity of DDAB with PVA modified zeolites are very close to that of corresponding parent NZ which indicates that the crystalline nature of the zeolites remained intact after modified. The relative intensity of mordenite characteristic peaks at 2θ of 9.87°, 13.58°, 19.74°, 22.29°, 25.73°, 26.71°,27.70°, 29.98° and 30.92°, increased due to

the cation exchange reaction which takes place in natural zeolites when they were modified by DDAB.

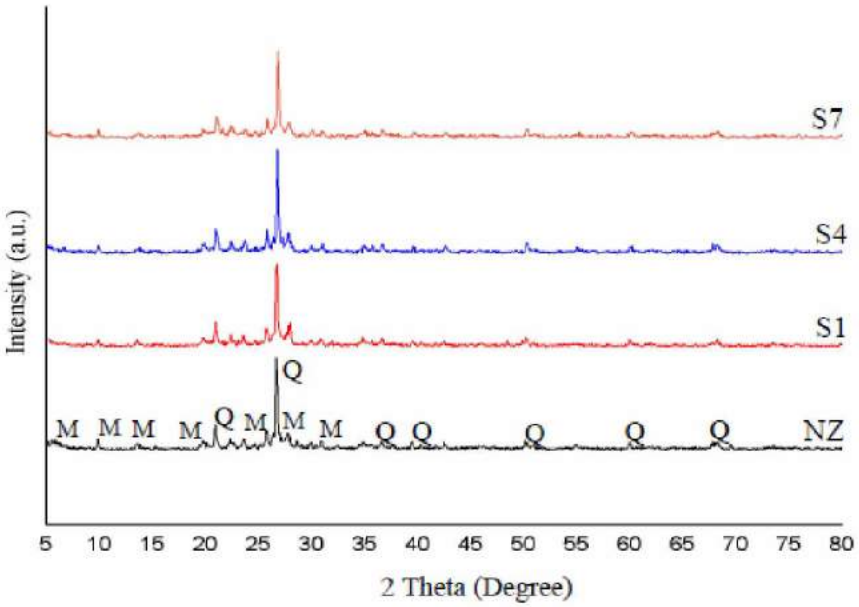

Figure 3.1: XRD pattern of NZ and SMGZ.

3.1.2 Fourier Transform Infrared Spectroscopy

FTIR spectra of the NZ, PVA, DDAB and SMGZ (S1, S4 and S7) are shown in **Figure 3.2**. The band observed at 3439 cm^{-1} is assigned to hydroxyl group of water. For the structure of zeolite T— O, asymmetric and symmetric stretching of T— O (T= Si or Al) are observed between 1038-608 cm^{-1}. Band at 532 cm^{-1} is assigned for double six rings for Si — O —T bonds of zeolite framework while band at 469 cm^{-1} is assigned for bending mode of T—O [32]. The presence of additional peaks at 2917-2850 cm^{-1} are caused by C— H stretching of hydrocarbon originating from the DDAB which is present on the SMGZ structure. The frequencies and widths of the CH_2 stretching modes depend strongly on the conformation and the packing density of methylene chains [32-34]. The presences PVA with NZ, as in S1, do not add any new banding which

indicates that the nature of the zeolites remained intact after granulation. Broadening of bands in SMGZs implied that DDAB molecules on the modified zeolites have a more disordered structure than the NZ.

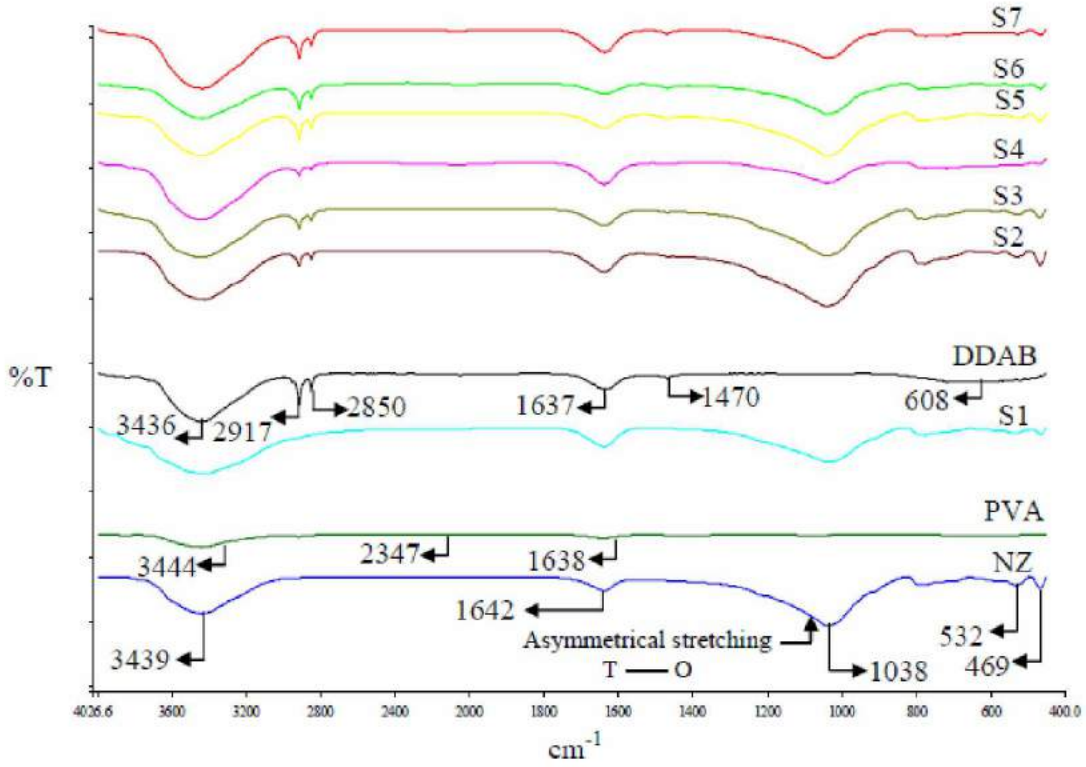

Figure 3.2: FTIR spectrum of NZ, PVA, DDAB and SMGZ (T= Si or Al).

3.1.3 Porosity and BET Specific Surface Area

The porous properties and surface area of the NZ and SMGZ were further investigated by the nitrogen adsorption-desorption isotherm and Barrett-Joyner-Halenda (BJH) methods. **Figure 3.3** shows the N_2 adsorption-desorption isotherm with the obvious hysteresis phenomenon and the pore-size distribution (inset) of the NZ, SMGZ-S1 and SMGZ-S4. Both NZ and SMGZ showed a type IV adsorption isotherm with an obvious hysteresis loop, signifying the presence of

mesopores (2-50 nm in size) in all samples [35- 36]. Moreover, it can be seen that the hysteresis loop shifts approach $P/P_0 = 1$, indicating the existence of macropores (>50 nm). The isotherm for NZ and SMGZ-S1 showed an obvious and light wide hysteresis loop at relative pressures of 0.45, which is distinctive for mesoporous zeolite of ink-bottle type pores with pore necks lesser than 4 nm (**Figure 3.3 a and b**) [37]. After modification (**Figure 3.3 c**) the vertical hysteresis loop of SMZ-S4 was closed of $P/P_0 = 0.40$ indicates the presence of mesopores volumes in SMZ-S4, and suggested the presence of cylindrical type pores [38].

According to the IUPAC recommendations, 65 hysteresis loops are classified into four types H1, H2, H3 and H4) [36]. From **Figure 3.3 (a) and (b)** the NZ and SMGZ-S1 have H4 while SMGZ-S4 has H1 (**Figure 3.3 c**).

The Type H1 loop shows parallel and nearly vertical branches. This kind of hysteresis loop was often reported for SMGZ-S4 that consisted of agglomerates (assemblages of rigidly joint particles) or compacts of approximately spherical particles arranged in a fairly uniform way. More recently, it has become clear that H1 hysteresis loops are also characteristic of materials with cylindrical pore geometry and a high degree of pore size uniformity. Therefore, the presence of the H1 hysteresis loop on the adsorption isotherm for a porous solid usually indicates its relatively high pore size uniformity and facile pore connectivity (**Table 3.1**).

Type H4 loops feature parallel and almost horizontal branches and their occurrence has been attributed to adsorption-desorption in narrow slit like pores. However, current experimental data for well defined systems question this interpretation. Moreover, the Type H4 loop was reported for NZ and SMGZ-S1 that exhibited particles with internal voids of irregular shape and broad size distribution (between 5 and 30 nm). Hollow spheres with walls composed of ordered mesoporous silica also showed hysteresis behavior of the H4 type. This would suggest that H4 hysteresis loops may merely arise due to the presence of large mesopores embedded in a matrix with pores of much smaller size (**Table 3.1**).

Otherwise, as shown in **Table 3.1** the BET surface area of NZ has not changed much after addition PVA (SMGZ-S1). Also the total pore volumes of NZ and SMGZ-S1 were found to be closed to each other. While the surface areas and pore volume of SMGZ-S2 has large changed when compared with other samples.

It was evident that the surface areas of NZ and SMGZ-S1 have decreased significantly and also pore volumes while pore size have increased after the modification with the cationic surfactant DDAB [36]. This is due to the presences of DDAB molecules on the zeolite surface, which hampered some of the main pore channels of natural zeolite, thus obstructing the diffusion of N_2 throughout these channels [39]. These results agree with those from results of FTIR which indicates the presence of PVA does not affect on structure of NZ.

Table 3.1: The porosity and specific surface areas of NZ, SMGZ-S1 and SMGZ-S4.

Sample	BET (m^2/g)	Pore volume (cm^3/g)	Pore size (Å)
NZ	23.9923	0.039179	65.3193
S1	26.9681	0.046057	68.3128
S4	6.6873	0.025749	154.0167

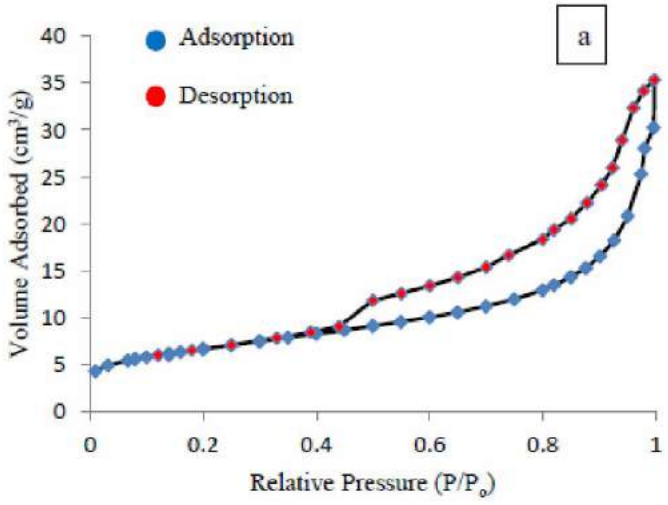

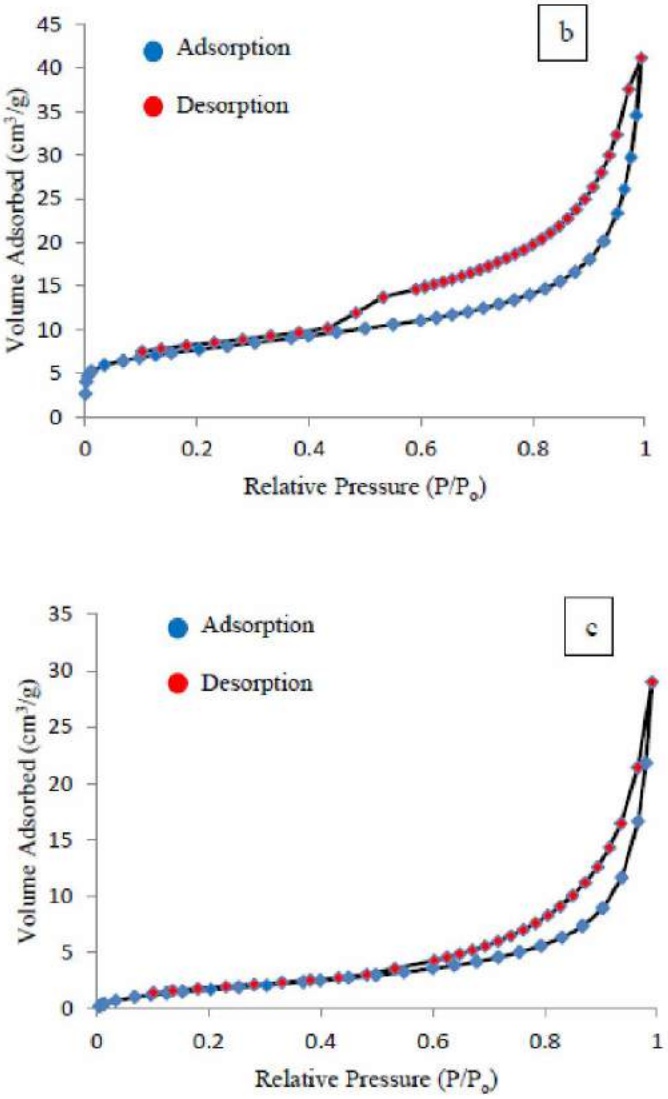

Figure 3.3: N_2 Adsorption–Desorption Isotherms for (a) NZ, (b) SMGZ-S1 and (c) SMGZ-S4.

3.1.4 FESEM micrographs and Elemental Analysis

The morphologies of the NZ, SMGZ-S1 and SMZS4 were captured using FESEM. The great difference in the surface morphology was observed. **Figure 3.4 (a)** exhibited a distinct flowery pattern with some sheet-like morphology for NZ. While the SMZ-S1 illustrates an image of a rough and uneven surface as a result of the addition of PVA to the NZ (**Figure 3.4 b**). On the other hand, **Figure 3.4 (a)** exhibited a semi-smooth surface. This result shows that an organic layer was formed on the surface of natural zeolite after being modified by DDAB.

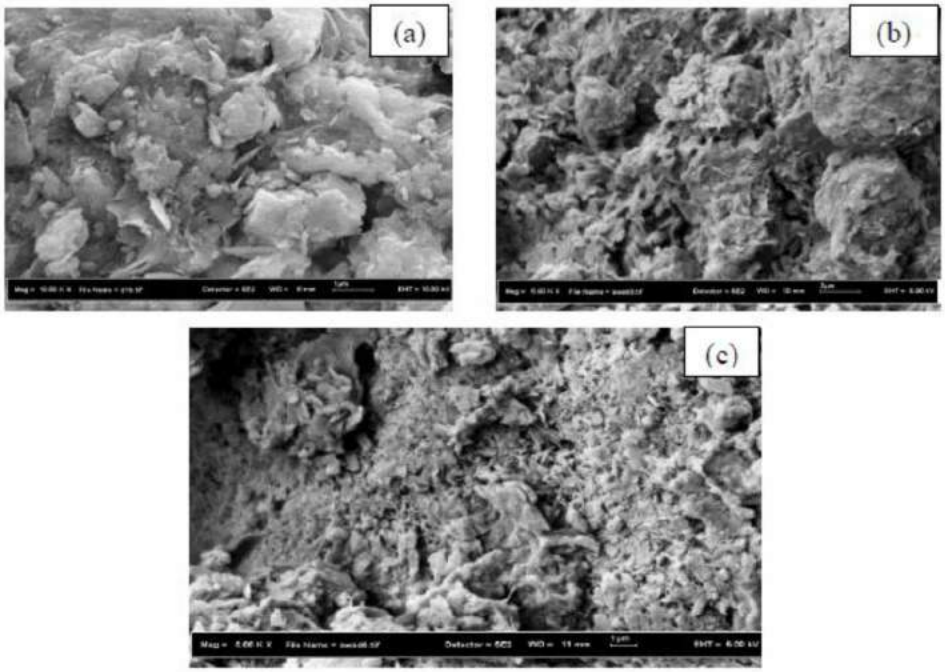

Figure 3.4: FESEM photographs (a) NZ, (b) SMGZ-S1and (c) SMGZ-S4

EDX is a surface analytical technique and the results of EDX elemental analysis are presented in **Table 3.2**. Since energy dispersive is less sensitive to elements with atomic numbers less than 20, the weight percents listed in the related tables in these figures has been calculated on an oxygen-free basis [40]. EDX is a surface analytical technique.

Table 3.2: EDX elemental analysis of NZ, SMZ-S1and SMGZ-S4

element	NZ (wt %)	SMZ-S1 (wt %)	SMZ-S4 (wt %)
C	0.00	4.15	22.40
Na	0.00	0.82	0.88
Si	28.45	25.55	22.72
Al	8.21	8.07	6.75
Mg	1.11	1.06	0.90
K	4.58	3.15	1.53
Fe	3.30	6.13	3.70
Si/Al	3.47	3.17	3.36

The elemental compositions obtained indicate that the elemental weight percentages of carbon ions increased from near zero in NZ to 4.15 % in SMZ-S1 and to 22.40 % which indicates the presence of PVA and DDAB. Moreover, the elemental weight percentages of potassium ions decreased while the iron ions increased at SMGZ-S1 then after that decreased with DDAB, which shows that ion exchange occurred for K^{+} and Fe^{++} rather than Na^{+}. The percentage of sodium and magnesium ions has not after modification. The percentage of Na^{+} in EDX spectrum of sample NZ is near to zero. Sodium ions included within the interparallel pore are more difficult to recover by ion exchange [41]. The larger pore size of SMGZ-S4 (86.17°A) provides a more facile passage for metal ions and increases its resulting exchange rate rather than NZ (154.0167 Å). The modified of NZ by DDAB results into increase of the interparallel size and decreased surface area, as a result, some of the available sodium ions are able to exchange with surface ions. Otherwise, the Si/Al ratio has a little decreased after modification.

3.2.1 Impact of DDAB and PVA loading levels

The adsorption of HA on granulate zeolite samples, S1 until S7, were studied using initial HA concentration (C_t) of 30 mg/L. As shown in **Figure 3.5**, SMGZ-S4 at the flow rate 18 mL/min displayed a higher uptake (q_e) of HA than other samples. The zero point of charge (zpc) shows at S4, 12% of DDAB. The formation of monolayer of surfactant (DDAB) which covered zeolite surface is

reason to increase the adsorption capacity of SMGZ-S4. The HA adsorption capacity of all samples also increased with increasing contact time. The total adsorbed amount, the maximum HA uptake and removal percent with respect to the different samples of SMGZ are presented in **Table 3.3**.

Table 3.3: Comparison of adsorption capacities on natural granular zeolite and SMGZ for removal of HA (initial concentration 30 mg L-1; flow rate 18 mL/min; solution pH 7.00).

Sample	C_{ad} (mg L^{-1})	q_{total} (mg)	q_e (mg g^{-1})	M_{total} (mg)	Y (%)
S1	22.20	39.96	00.27	54	74
S2	25.80	46.44	00.31	54	86
S3	28.50	51.30	00.34	54	95
S4	29.70	53.46	00.36	54	99
S5	28.80	51.84	00.35	54	96
S6	28.20	50.76	00.34	54	94
S7	27.60	49.68	00.33	54	92

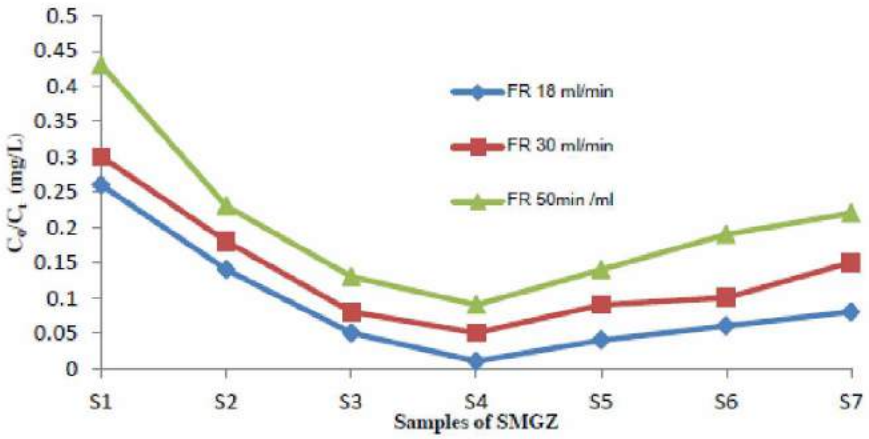

Figure 3.5: Adsorption of HA by SMGZ at various feed flow rate and pH 7.00

3.2.2 Impact of solution flow rate

The result with bed volume at different flow rates was determined at diverse DDAB loading level. The penetration curves were obtained as HA concentrations in the effluent versus SMGZ for various feed flow rates and are presented in **Figure 3.5**. The breakthrough point in the system occurred at S4 for all flow rates of 18, 30 and 50 mL min^{-1}. The lower feed flow rates flow rates display more effectual adsorption of HA than the higher once. The minimum feed flow rate produce more efficient removal of HA than the maximum ones as a result of the higher empty bed contact time (EBCT) of the previous one, which include sufficient mass transfer.

3.2.3 Effect of pH on HA adsorption onto SMGZ

Figure 3.6 indicates the behavior of HA adsorption onto SMGZ as a function of pH, exhibiting a higher uptake of HA occurred at pH 7.00. **Figure 3.6** shows that the total HA removal efficiency at SMGZ-S4 increased from 94 % to 99 % with the increase of pH from 4 to 7, thereafter it reduced to around 96% when water's pH was elevated to 10 under flow rate 18 mL min^{-1}. This contradiction in behavior can be related to the difference in the adsorbent as well as in the experimental circumstances. The conduct of HA adsorption as a function of water's pH can be illustrated by considering the change in density of hydrogen ions, zeta potential of HA molecules, and the surface charge of zeolite as a function of water's pH. Through previous studies [42] found that zeolite particle's surface is uncharged at water pH about of 7.00; zeolite particle's surface has positive charge at water pH below 7.00, and it is negatively charged at water pH above 7.00.

Influence of pH on adsorption of HA can be explained by the fact that HA has a negative zeta potential at pH above 2 [42]. The increase the pH is, the greater would be the negativity of the HA molecules, and thus the increase would be the attraction force between negatively charged HA molecules with the positively charged surface of SMGZ up to pH 7.00. At pH about 8.00, the surface of SMGZ had no charge which led to decrease of attraction force and in turn resulted in decrease of HA adsorption. Furthermore, the surface of SMGZ had a

negative charge for pHs more than 8.00, while HA molecules were negatively charged at these pHs. This led to domination of repulsion forces over attraction ones and thus lessening of adsorption rate. In addition, this can be explained by considering the variation in ionic charge of HA as well as the pHzpc of zeolite, and thus the variation in removal mechanism. In fact, SMGZ are positively charged whereas the HA is an anionic hydrophobic compound. Therefore, the HA might be removed by mechanism of electrostatic attraction of humate anions to the positively charged sites on the SMGZ. Certainly, the HA molecules were adsorbed onto positively charged sites on the surface of SMGZ through electrostatic attraction forces between phenolic and/or carboxylic groups of HA with the cations surfactant on the NZ.

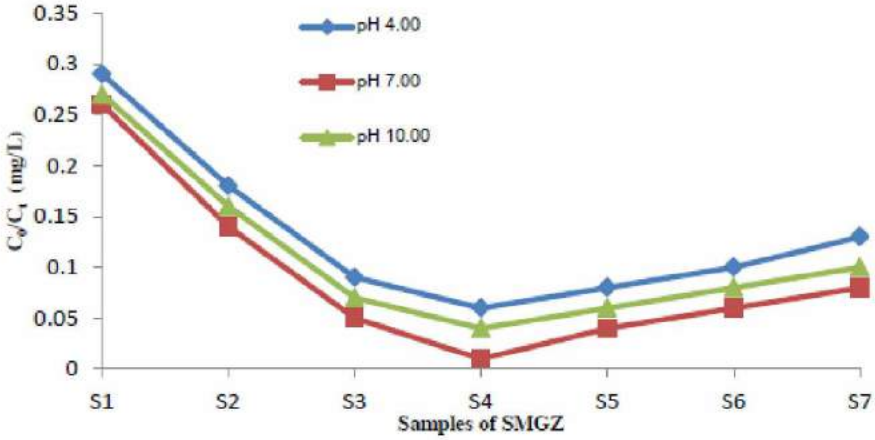

Figure 3.6: Effects of solution pH on HA adsorption onto SMGZ at flow rate 18 ml/min

4.0 CONCLUSIONS

Natural granular zeolite mostly has low adsorption efficiency to HA from water, but DDAB modification can certainly change the adsorption characteristics of the zeolite for HA. The HA adsorption efficiency was found to be dependent on DDAB loading amounts, flow rate, solution pH. The SMGZ-S4 at 12% of DDAB

and the minimum flow rate (18 mL min^{-1}) were found to exhibit the best performance for the adsorption of HA. The maximum adsorption of humic acid was obtained at pH ranges of natural water's pH. It is proposed that monolayer formation favours the interaction of HA and DDAB covered zeolite surface. The general conclusion of this work is that HA adsorption on SMGZ surfaces is mainly as a result of the hydrophobic interaction, hydrogen bonding and partitioning mechanism.

REFERENCES

[1] Rao, P. et al (2011). Removal of natural organic matter by cationic hydrogel with magnetic properties. *J. of Envir Manag.*, 92, 1690-1695.
[2] Lin, J. et al (2012). Adsorption of humic acid from aqueous solution onto unmodified and surfactant-modified chitosan/zeolite composites. *Chem. Eng. J.*, 200–202, 202-213.
[3] Wang, S. et al (2008). Adsorption of Cu(II), Pb(II) and humic acid on natural zeolite tuff in single and binary systems. *Separation and Purification Technology*, 62, 64-70.
[4] Ding, C. and Shang, C. (2010). Mechanisms controlling adsorption of natural organic matter on surfactant-modified iron oxide-coated sand. *Water Research*, 44, 3651-3658.
[5] Yang, J.et al (2004). Removal of fulvic acid from water electrochemically using active carbon fiber electrode. *Water Research*, 38, 4353-4360.
[6] Yang, X. et al (2007). Factors affecting formation of haloacetonitriles, haloketones, chloropicrin and cyanogen halides during chloramination. *Water Research*, 41, 1193-1200.
[7] Matilainen, A. and Sillanpää, M. (2010). Removal of natural organic matter from drinking water by advanced oxidation processes. *Chemosphere*, 80, 351-365.
[8] A. Imyim, E. Prapalimrungsi(2010). Humic acids removal from water by aminopropyl functionalized rice husk ash, *J.Hazard. Mater.* 184, 775–781.
[9] Tao, Q. et al (2010). Adsorption of humic acid to aminopropyl functionalized SBA-15, *Micropor. Mesopor. Mater.* 131, 177–185.
[10] Li, C.J. et al (2011). Surfactant modified zeolite as adsorbent for removal of humic acid from water, *Appl. Clay Sci.* 52, 353–357.
[11] Hartono, T. et al (200). structured graphite oxide as a novel adsorbent for humic acid removal from aqueous solution, J. Colloid Interface Sci. 333, 114–119.
[12] Wang, M.S. et al (2011). Adsorption of low concentration humic acid from water by palygorskite, *Appl. Clay Sci.* 1016,09-012.
[13] Wang, J.H. et al (2011). Adsorptive removal of humic acid from aqueous solution on polyaniline/attapulgite composite, *Chem. Eng. J.* 173, 171–177.
[14] Jarvis, K.L. and Majewski, P. (2012). Plasma polymerized allylamine coated quartz particles for humic acid removal, *J. Colloid Interface Sci.* 380, 150–158.
[15] Stˇrek, A. et al (1994). Comparison of the adsorption of humic acids from aqueous solutions on active carbon and activated charcoal cloths, *Carbon*. 32, 207–211.
[16] Wang, S. and Peng, Y. (2010). Natural zeolites as effective adsorbents in water and wastewater treatment. *Chem. Eng. J.* 156, 11-24.

[17] Wang S. and Peng Y. (2010). Natural zeolites as effective adsorbents in water and wastewater treatment. *J.Chemical Engineering* , 156, 11-24.

[18] Yang, S. et al (2011). Determination of Ni(II) uptake mechanisms on mordenite surfaces: A combined macroscopic and microscopic approach. *Geochimica et Cosmochimica Acta*. 75, 6520-6534.

[19] Bajpai, P. K. (1986). Synthesis of mordenite type zeolite. *Zeolites*. 6, 2-8.

[20] Arletti, R., et al (2012). Location of MTBE and toluene in the channel system of the zeolite mordenite: Adsorption and host–guest interactions. *J. Solid State Chem*., 194, 135-142.

[21] Knappe, D.R.U. and Rossner, A. (2005). Effectiveness of high silica zeolites for the adsorption of methyl tertiary-butyl ether from natural water, *Water Sci. Technol.: Water supply*. 5, 83–91.

[22] Hung, H.-W. and Lin, T.-F. (2006). Adsorption of MTBE from contaminated water by carbonaceous resins and mordenite zeolite, *J. Hazard. Mater*. 135, 210–217.

[23] Li, S. et al (2003). MTBE adsorption on all-silica - zeolite, *Environ. Sci. Technol*. 37, 4007–4010.

[24] Abu-Laila, Laila et al (2010). Adsorption of methyl tertiary butyl ether on granular zeolites:Batch and column studies, *J. Hazard.Mater*. 178, 363–369.

[25] Wilson M.J. (1994). Clay mineralogy: Spectroscopic and chemical determinative method. Great Britain, Chapman & Hall.

[26] Aksu, Z. and Gonen F. (2004). Biosorption of phenol by immobilized activated sludge in a continuous packed bed: prediction of breakthrough curves, *Process Biochem*. 39, 599–613.

[27] Han, R. et al. (2009). Adsorption of methylene blue by phoenix tree leaf powder in a fixed-bed column: experiments and prediction of breakthrough curves. *Desalination*. 245, 284-297.

[28] Wan Ngah, W. S. et al (2012). Utilization of chitosan–zeolite composite in the removal of Cu(II) from aqueous solution: Adsorption, desorption and fixed bed column studies. *Chem. Eng. J*. 209, 46-53.

[29] Yin, C. Y. et al (2009). Fixed-bed adsorption of metal ions from aqueous solution on polyethyleneimine-impregnated palm shell activated carbon. *Chem. Eng. J*. 148, 8-14.

[30] Han, R. et al (2009). Characterization and properties of iron oxide-coated zeolite as adsorbent for removal of copper(II) from solution in fixed bed column. Chem. Eng. J. 149, 123-131.

[31] Castaldi, P. et al (2008). Sorption processes and XRD analysis of a natural zeolite exchanged with Pb2+, Cd2+ and Zn2+ cations. *J. Hazard. Mate*. 156, 428-434.

[32] Elaiopoulos, K. et al (2010). Monitoring the effect of hydrothermal treatments on the structure of a natural zeolite through a combined XRD, FTIR, XRF, SEM and N_2-porosimetry analysis. *Microporous and Mesoporous Materials*. 134, 29–43.

[33] Rozic, M. et al (2009). Sorption phenomena of modification of clinoptilolite tuffs by surfactant cations. *J. Colloid Interface Sci*. 331, 295–301.

[34] Vaia, R. A. et al. (1994). Interlayer structure and molecular environment of alkylammonium layered silicates. *Chem. Mater*. 6, 1017–1022.

[35] Zhang, W. et al. (2012). Synthesis, surface group modification of 3D MnV2O6 nanostructures and adsorption effect on Rhodamine B. *Materials Research Bulletin*, 47, 1725-1733.

[36] Kruk, M. and Jaroniec, M. (2001). Gas Adsorption Characterization of Ordered Organic−Inorganic Nanocomposite Materials. *Chemistry of Materials*. 13, 3169-3183.

[37] Qin, Z. et al. (2011). Mesoporous Y zeolite with homogeneous aluminum distribution obtained by sequential desilication–dealumination and its performance in the catalytic cracking of cumene and 1,3,5-triisopropylbenzene. J.Catalysis. 278, 266-275.

[38] Kim, K.J. and Ahn, H.G. (2012). The effect of pore structure of zeolite on the adsorption of VOCs and their desorption properties by microwave heating. *Microporous and Mesoporous Materials*. 152, 78-83.

[39] Leyva-Ramos, R. et al. (2008). Adsorption of chromium(VI) from an aqueous solution on a surfactant-modified zeolite. Colloids and Surfaces A: *Physicochemical and Engineering Aspects*. 330, 35-41.

[40] Shams, K. and Mirmohammadi, S. J. (2007). Preparation of 5A zeolite monolith granular extrudates using kaolin: Investigation of the effect of binder on sieving/adsorption properties using a mixture of linear and branched paraffin hydrocarbons. *Microporous and Mesoporous Materials*. 106, 268-277.

[41] Shams, K. and Ahi, H. (2013). Synthesis of 5A zeolite nanocrystals using kaolin via nanoemulsion-ultrasonic technique and study of its sorption using a known kerosene cut. *Microporous and Mesoporous Materials*. 180, 61-70.

[42] Moussavi, G. et al. (2011). The investigation of mechanism, kinetic and isotherm of ammonia and humic acid co-adsorption onto natural zeolite. *Chem. Eng. J.* 171, 1159-1169.